European Radiology (2019) 29:3820–3829
https://doi.org/10.1007/s00330-018-5981-2

BREAST

Radiomic nomogram for prediction of axillary lymph node metastasis in breast cancer

Lu Han[1,2] · Yongbei Zhu[3] · Zhenyu Liu[3,4] · Tao Yu[1,2] · Cuiju He[1,2] · Wenyan Jiang[1,2] · Yangyang Kan[1,2] · Di Dong[3,4] · Jie Tian[3,4,5] · Yahong Luo[1,2]

Received: 24 October 2018 / Accepted: 17 December 2018 / Published online: 30 January 2019

Abstract

Objective To develop a radiomic nomogram for preoperative prediction of axillary lymph node (LN) metastasis in breast cancer patients.

Methods Preoperative magnetic resonance imaging data from 411 breast cancer patients was studied. Patients were assigned to either a training cohort ($n = 279$) or a validation cohort ($n = 132$). Eight hundred eight radiomic features were extracted from the first phase of T1-DCE images. A support vector machine was used to develop a radiomic signature, and logistic regression was used to develop a nomogram.

Results The radiomic signature based on 12 LN status–related features was constructed to predict LN metastasis, its prediction ability was moderate, with an area under the curve (AUC) of 0.76 and 0.78 in training and validation cohorts, respectively. Based on a radiomic signature and clinical features, a nomogram was developed and showed excellent predictive ability for LN metastasis (AUC 0.84 and 0.87 in training and validation sets, respectively). Another radiomic signature was constructed to distinguish the number of metastatic LNs (less than 2 positive nodes/more than 2 positive nodes), which also showed moderate performance (AUC 0.79).

Conclusions We developed a nomogram and a radiomic signature that can be used to identify LN metastasis and distinguish the number of metastatic LNs (less than 2 positive nodes/more than 2 positive nodes). Both nomogram and radiomic signature can be used as tools to assist clinicians in assessing LN metastasis in breast cancer patients.

Key Points

- *ALNM is an important factor affecting breast cancer patients' treatment and prognosis.*
- *Traditional imaging examinations have limited value for evaluating axillary LNs status.*
- *We developed a radiomic nomogram based on MR imagings to predict LN metastasis.*

Keywords Breast cancer · Axillary lymph node metastasis · Radiomics · Preoperative prediction · MRI

Lu Han and Yongbei Zhu contributed equally as the first authors.

✉ Di Dong
di.dong@ia.ac.cn

✉ Yahong Luo
Luoyahong8888@hotmail.com

[1] Cancer Hospital of China Medical University, Shenyang 110042, China

[2] Liaoning Cancer Hospital & Institute, Shenyang 110042, China

[3] CAS Key Laboratory of Molecular Imaging, Chinese Academy of Sciences, Institute of Automation, Beijing 100190, China

[4] University of Chinese Academy of Sciences, Beijing 100049, China

[5] Beijing Advanced Innovation Center for Big Data-Based Precision Medicine, Beihang University, Beijing 100191, China

Abbreviations

ALND	Axillary lymph node dissection
ALNM	Axillary lymph node metastasis
AUC	Area under the curve
CI	Confidence interval
ER	Estrogen receptor
GLCM	Gray level co-occurrence matrix
GLRLM	Gray level run length matrix
GLSZM	Gray level size zone matrix
HER2	Human epidermal growth factor receptor 2
LN	Lymph node
PR	Progesterone receptor
ROC	Receiver operating characteristic
SLNB	Sentinel lymph node biopsy

T1-DCE T1-weighted images of dynamic contrast enhanced

Introduction

Breast cancer is the second most common malignant tumor all over the world, and the incidence rate ranks first among cancers in women. Approximately 1.67 million new breast cancer cases were diagnosed worldwide, accounting for a quarter of all cancers in 2012 [1]. General trends indicate that although the incidence of breast cancer is increasing, mortality is decreasing, while in China, breast cancer's mortality rate is slightly increasing [2]. There are many elements that can affect the prognosis in breast cancer patients, including tumor size, the degree of axillary lymph node metastasis (ALNM), histological subtype and grade, and the presence of lymphovascular invasion [3]. Among these factors, tumor size and the degree of ALNM can be evaluated non-invasively.

Clinicians once regarded that breast cancer's standard treatment was radical mastectomy plus axillary lymph node dissection (ALND) because it was thought that the tumor cells begin locally, spreading to regional lymph node (LN), and then to distant tissues [4]. However, owing to the aggressive and extensive nature of the surgery, ALND is associated with considerable complications, including lymphedema, infection, limitation of shoulder motion, and major vessel and nerve injury [5, 6]. By contrast, sentinel lymph node biopsy (SLNB) is selective resection of the first lymph node receiving lymphatic drainage straightly from the primary tumor. Because of this, SLNB is an alternative to routine ALND [7], and the complications associated with SLNB are less extensive compared with ALND [8].

Examinations such as physical examination, mammography, ultrasonography, and MRI are all commonly used to diagnose breast cancer; however, their abilities to assess LNs are limited [9–15]. MRI has been widely used in breast cancer patients to discriminate benign versus malignant disease, define the extent of lesions, detect contralateral, and occult disease [16]. In addition, MRI has been recommended for screening for high-risk women [17]. However, as the limited power of traditional examinations for evaluating ALNM, developing an appropriate and non-invasive approach for assessing ALNM has been a challenge.

Radiomics is a arising field that involves converting digital medical images into mineable data, analyzing data, and improving medical decision, which may enhance accuracy of diagnosis, prognosis, and prediction, especially in oncology [18–20]. The field of breast MRI radiomics is growing rapidly, mainly focusing on the identifying benign and malignant tumors [21], analyzing molecular subtypes [22], and predicting chemotherapy response [23].

Axillary LN staging and treatment has been a hot topic of research. ALND has been considered the standard treatment for breast cancer for some time, but it was associated with both short- and long-term morbidities. A trial from the American College of Surgeons Oncology Group Z0011 [24] showed that for breast cancer patients accompanied one to two metastatic sentinel LNs who accept breast conserving surgery and systemic therapy, there was no survival benefit associated with ALND compared with SLNB. In addition, 2014 American Society for Clinical Oncology (ASCO) guidelines [25] recommend that early stage breast cancer patients with one or two sentinel LN metastases should not be recommended to accept ALND, and they should undergo breast conserving surgery and whole breast radiotherapy. Based on the results of the Z0011 trials and ASCO guidelines, in this study, we attempted to find whether the number of metastatic LNs can be predicted through radiomics.

The purpose of our study was to develop a radiomic nomogram for predicting ALNM based on MR images.

Materials and methods

Patients

This study was approved by the ethics committee. We retrospectively evaluated breast cancer patients treated in our hospital between January and July of 2016. Inclusion criteria for the study included having (1) histologically confirmed breast cancer; (2) all patients underwent SLNB or ALND, when SLNB was positive, complete ALND was performed; (3) underwent dynamic contrast enhanced MRI examination before surgery; and (4) access to clinical characteristics.

The exclusion criteria included a history of (1) preoperative radiotherapy, chemotherapy, or endocrine therapy; (2) ipsilateral breast surgery; or (3) distant metastasis. Four hundred eleven patients were enrolled in this study. Patients treated between January and May were assigned to a training cohort ($n = 279$) and patients treated between June and July were assigned to a validation cohort ($n = 132$).

Clinical characteristics

Clinical characteristics including LN status (LN with macrometastasis or micrometastasis was considered positive), the number of metastatic LNs, status of human epidermal growth factor receptor 2 (HER2), estrogen receptor (ER), progesterone receptor (PR), KI-67 levels, and histological tumor type were obtained by reviewing patients' pathology reports. Tumors were considered ER or PR positive if 10% or more immunostained cells. Hematoxylin-eosin (HE) staining at least 3+ is defined as HER2 positive, and positivity of KI-67 was defined as at least 14% immunostained cells. Clinical data

such as age and physical examination were obtained from patients' medical records.

MR image acquisition and MRI-reported LN status

All images were obtained by a 1.5 T MRI system (HDx, GE Healthcare), using an 8-channel breast dedicated coil in prone position. T1-weighted images of dynamic contrast enhanced (T1-DCE) MR images were analyzed for this study. The contrast agent was injected intravenously (0.1 mmol/kg of Gd-DTPA-MBA, Omniscan, GE Healthcare), then followed by a 20-mL saline flush, both at a rate of 3 ml/s. After intravenous injection, continuous non-interval scans were performed in eight phases, with a scan time for each phase of 43 s, for a total scan time of 5.7 min. Parameters for MRI scans were as follows: axially VIBRANT sequence (a 3D T1-weighted imaging technique that performs bilateral breasts conventional scans or dynamic enhanced scans to obtain axial or sagittal breast images with high signal-to-noise ratio and high resolution) with a repetition time/echo time: 6.2/3.0 ms; flip angle: 10°; slice thickness: 3.2 mm; 48 slices per volume; the field of view: 360 × 360 mm; matrix size: 256 × 256. These parameters were identical for every patient. All breast MRI exams include complete FOV of the axillary region. Two radiologists reviewed all images, one with 5 years of breast cancer MRI interpretation experience and the other with 10 years of breast cancer MRI interpretation experience. Each radiologist recorded the number of lesions, tumor size (the maximum in-plane diameter of the largest lesion), and MRI-reported LN status (a LN was believed suspicious when it had one of the following characteristics: circular shape, missing fatty hilum, or eccentric cortical thickening [26]). In the case where radiologists disagreed about the status of LN, consensus was reached through discussion. If more than one lesion was noted, we defined it as multifocality.

MRI data processing and analysis

A flowchart (Fig. 1) illustrating the radiomic method for predicting LN metastasis consisted of image segmentation, high-throughput feature extraction, feature selection, and the development of predictive models.

ROI segmentation

Manual segmentation was performed on axial first phase of T1-weighted images of dynamic contrast enhanced (T1-DCE) images. First, the tumor lesion area was delineated using freely available software (ITK-SNAP; http://www.itksnap.org). Lesions were delineated by a radiologist with 5-year experience with no information about the tumor's histological type or the patient's LN status.

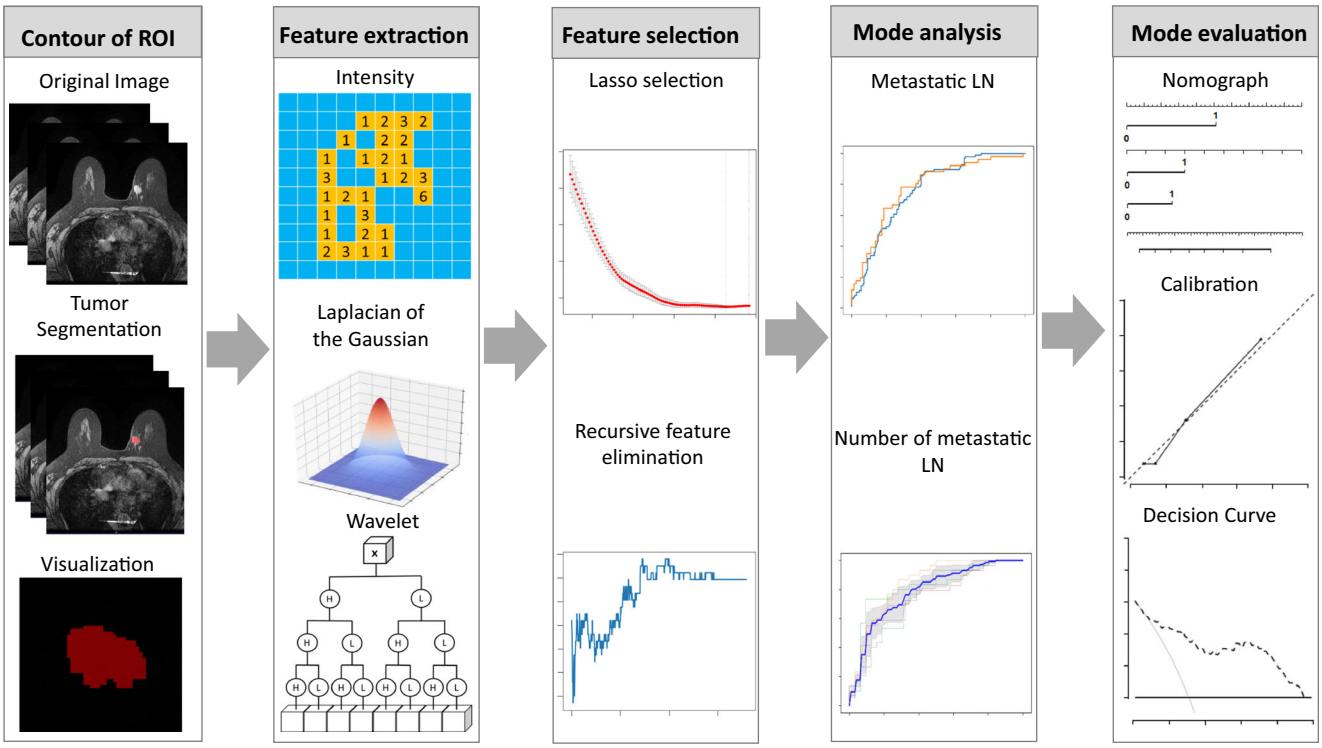

Fig. 1 Radiomics workflow

Table 1 Clinical characteristics

Characteristics	LN-metastasis group ($n = 148$)	Non-LN-metastasis group ($n = 263$)	p value	Training cohort ($n = 279$)	Validation cohort ($n = 132$)	p value
Age (mean ± SD)	52.37 ± 9.7	51.87 ± 9.4	0.612	52.10 ± 9.7	51.95 ± 10.4	0.890
Tumor size on MRI (mm)	20.08 ± 8.5	19.07 ± 9.0	0.264	19.56 ± 8.5	19.17 ± 9.4	0.670
Histologic type[#]			< 0.001			0.186
Precursor lesions	2	31		19	14	
Invasive carcinoma	146	231		259	118	
Other*	0	1		1	0	
Estrogen receptor status			0.059			0.228
Negative	40	95		97	38	
Positive	108	168		182	94	
Progesterone receptor status			0.977			0.122
Negative	70	124		139	55	
Positive	78	139		140	77	
HER2 status			0.877			0.262
Negative	118	208		217	109	
Positive	30	55		62	23	
KI-67 status			0.065			0.292
Negative	23	61		53	31	
Positive	125	202		226	101	
LN palpability			< 0.001			0.941
Yes	29	9		26	12	
No	119	254		253	120	
Multifocality			< 0.001			0.353
Yes	32	24		35	21	
No	116	239		244	111	
MRI-reported LN status			< 0.001			0.666
Negative	54	236		195	95	
Positive	94	27		84	37	
LN metastasis						
Yes				97	51	0.445
No				182	81	

[#] According to current guidelines [28] from the World Health Organization (WHO) on the classification of breast tumors, histologic tumor types in this study were categorized as (1) precursor lesions (including 32 ductal carcinomas in situ and 1 lobular carcinoma in situ with ductal carcinoma in situ), (2) invasive carcinomas (including 350 invasive carcinomas of no special type, 11 invasive lobular carcinomas, 4 invasive micropapillary carcinomas, 5 mucinous carcinomas, 1 medullary carcinoma, 1 invasive carcinoma of no special type with medullary features, 1 cribriform carcinoma, and 3 carcinoma with neuroendocrine features, and 1 carcinoma with apocrine differentiation), and (3) other (including 1 solid papillary carcinoma)

*Because data in this row is too small for analysis by itself, this data put it into "invasive carcinoma" group, and then analyzed

Feature extraction

A total of 808 radiomic features, consisting of 16 shape features, 19 first-order statistical features, 69 textural features for the original image set, and first-order statistical and textural features for eight wavelet filtered image sets, were extracted. Radiomic features were extracted using open-source software (Pyradiomics; http://pyradiomics.readthedocs.io/en/latest/index.html#) [27].

Feature selection

To reduce irrelevant and redundant information, a two-stage feature selection was performed in the training cohort. First, Mann-Whitney U tests were performed, and features with $p < 0.1$ were selected as potentially informative features. Next, two selection models were used to select optimal features. The first model (a least absolute shrinkage and selection operator (LASSO) regression model) works by shrinking the

Table 2 LN status–related features

First-order feature	Shape feature	GLCM	GLSZM	GLRLM
Median	Surface area to volume ratio	Informal measure of correlation (IMC)1	Size zone non-uniformity normalized (SZNN) (HLL)	Short run emphasis (SRE)
Robust mean absolute deviation		Entropy	Size zone non-uniformity normalized (SZNN) (LHH)	
Range		Sum entropy	Large area low gray level emphasis (LALGLE)	
		Sum average		

GLCM gray level co-occurrence matrix, *GLSZM* gray level size zone matrix, *GLRLM* gray level run length matrix

coefficients of useless features to zero with the regulation parameter λ in the training cohort. A second model (the leave-one-out cross-validation (LOOCV) method) was used to select the optimal regulation parameter for λ using 1-SE rule. Thus, features with a non-zero coefficient in the model with an optimal regulation parameter for λ were regarded as the most representative features. To build a reasonably stable model, a minimum of 15 observations per predictor variable were required. In addition, a recursive feature elimination (RFE) estimator that assigns weights to features was used to select the most useful predictive features. In cases where models selected too many features, sequential forward selection (SFS) was performed to avoid over-fitting. Selection models were implemented using Python software, Version 2.7 "scklearn" (Python Foundation for Statistical Computing).

Prediction nomogram construction

Radiomic signature

A linear support vector machine (SVM) was used to predict LN metastasis based on the selected MRI features identified in the training cohort. Sixfold validation was used to determine the optimal regulation parameter "C," which was designed to balance the need for diagnostic accuracy while avoiding an overly complex model in the training cohort. When the optimal value for C had been found, the radiomic signature based on the selected features was fitted to the training cohort and further validated in the validation cohort.

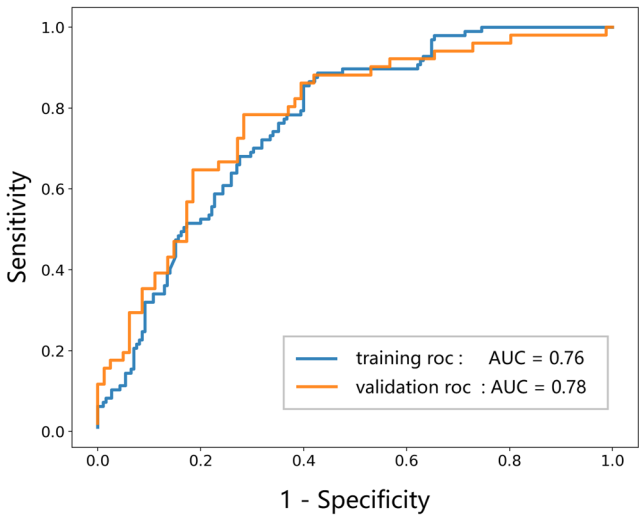

Fig. 2 ROC curve of radiomic signature for prediction LN metastasis in the training and validation cohorts

Clinical model

The association between LN metastasis and conventional clinical risk factors was assessed using univariate analyses. Based on the clinical factors with $p < 0.05$ in the univariate analyses, multivariate analyses used forward selection logistic regression (LR) to build the clinical model in the training cohort. The performance of the clinical model was then validated in the validation set.

Combined model

Incorporating the radiomic features in the best radiomic signature and the clinical factors in the clinical model, the combined model was built using the LR method. The performance of the combined model was then validated in the validation cohort. Receiver operating characteristic (ROC) curve and AUC were used to evaluate the performance of the above models. The Delong test was used to compare the combined model with the clinical model according to AUC values.

Nomogram establishment

To provide the clinicians and patients an individualized and easy-to-use tool for LN metastasis prediction, a nomogram for the clinical and combined models was plotted. The agreement between the LN metastasis predictions and the actual outcomes was assessed using a calibration curve. In addition, the Hosmer–Lemeshow test was used to assess the performance of the clinical and combined nomogram.

Table 3 Multivariable logistic regression analysis of risk factors for LN metastasis

Characteristic	Nomogram			
	β	Odds ratios (95%CI)		p value
Radiomics score	4.725897	7.8144 (3.999500–15.2680)		< 0.0001
MR reported LN status	2.055972	3.6011 (2.204100–5.8837)		< 0.0001
LN palpability	1.186217	3.2747 (1.062600–10.0920)		0.0389
	AUC	Sensitivity	Specificity	Accuracy
Training cohort	0.8388 (0.7887–0.8888)	0.6042	0.9382	0.8212
Validation cohort	0.8735 (0.7927–0.9542)	0.8529	0.8026	0.8182

Statistical analysis

Using R, Version 3.4.1 to perform statistical analyses For continuous clinical variables, Levene's test was used to assess the equality of variances between LN-metastasis group and non-LN-metastasis group, and Welch's t tests or Student's t tests were used to test between-group differences. For categorical variables, using Pearson's chi-squared tests to test differences between groups. For all tests, $p < 0.05$ was thought statistically significant.

Results

Clinical characteristics

Among the 411 patients, we analyzed 148 patients with LN metastasis and 263 patients without. The clinical characteristics of patients in the LN-metastasis group, non-LN-metastasis group, training cohort, and validation cohort are listed in Table 1. Statistical differences were found between LN-metastasis group and non-LN-metastasis group in histological type, LN palpability, multifocality, and MRI-reported LN status. The clinical characteristics of patients between the training set and the validation set have no statistical difference.

Radiomic signature building

Eight hundred eight features were extracted from T1-DCE images from the primary cohort, which were reduced to 12 LN status–related features, including 3 first-order features, 1 shape feature, 4 gray level co-occurrence matrix (GLCM) features, 3 gray level size zone matrix (GLSZM) features, and 1 gray level run length matrix (GLRLM) feature. Detailed information on these LN status–related features is available in Table 2. A radiomic signature containing 12 LN status–related features was constructed. The prediction performance of the radiomic signature was moderate, with an AUC of 0.76 (95% CI [0.76, 0.77]) in the training cohort and 0.78 (95% CI [0.77, 0.80]) in the validation cohort (Fig. 2). The sensitivity of the radiomic signature was good, as high as 89% and 78% in the training and validation cohorts, but the specificity was poor, only 57% and 72% in the training and validation cohorts. The

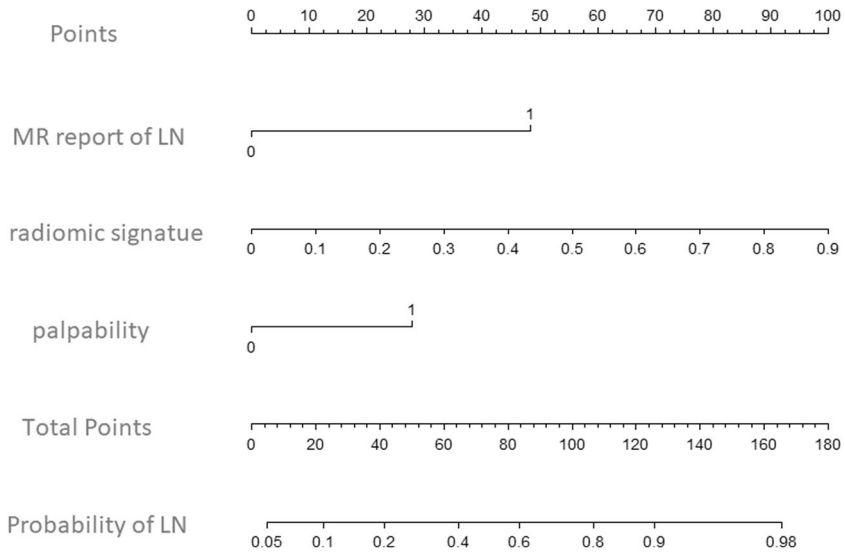

Fig. 3 Nomogram for prediction of LN metastasis. The different values for each variable corresponds to a point at the top of the graph, while the sum of the points for all the variables corresponds to a total point, draw a line from the total points to the bottom line is the probability of LN metastasis

accuracies were 72% and 70% in the training and validation cohorts, respectively.

Construction of the radiomic nomogram

Radiomic signature and clinical characteristics which showed significant differences when compared using Pearson's chi-squared tests were analyzed using multivariable logistic regression. Radiomic signature, MRI-reported LN status, and LN palpability were all discovered as independent risks for LN metastasis in the multivariable logistic regression model (Table 3). We developed a nomogram based on a radiomic signature, MRI-reported LN status, and LN palpability (Fig. 3). The calibration curve for the nomogram was tested using Hosmer-Lemeshow test, and yielded a non-significant result ($p = 0.11$ and 0.75 in training and validation cohorts, respectively) providing evidence of good calibration (Fig. 4a and b). The nomogram displayed an AUC of 0.84 (95% CI [0.79, 0.89]) for predicting LN metastases in the training cohort, and the sensitivity, specificity, and accuracy were 60%, 94%, and 82%, respectively. In the validation cohort, it also displayed excellent prediction efficacy, with an AUC of 0.87 (95% CI [0.79, 0.95]), and the sensitivity, specificity, and accuracy were 85%, 80%, and 82%, respectively.

Distinguishing the number of metastatic LNs

Eleven LN number–related features were selected from 808 possible features which were extracted from T1-DCE images of LN metastasis group, containing 2 first-order features, 1 shape feature, 4 GLCM features, 2 GLSZM features, and 2 GLRLM features. Detailed information on these LN number–related features were showed in Table 4. Based on these features, we developed a radiomic signature to distinguish the number of metastatic LNs (less than or equal to 2 and more than 2), and the distinguishing performance was moderate, with a mean AUC of 0.79 (Fig. 5). The sensitivity, specificity and accuracy were 80%, 64%, and 73%, respectively.

Clinical use

The decision curve analysis for the nomogram was showed in Fig. 6. The decision curve analysis indicated that when the threshold probability is within a range from 0.12 to 0.95, the net benefit of using nomogram to predict LN metastasis is greater than treat-all or treat-none scheme.

Discussion

In this study, we developed a nomogram based on a radiomic signature and clinical characteristics to predict LN metastasis, and it displayed excellent ability to predict LN metastases with an AUC of 0.87 in the validation cohort. In addition, we constructed a radiomic signature for distinguishing the number of metastatic LNs (less than or equal to 2 and more than 2), which also displayed good performance (AUC 0.79). Both of the nomogram and the radiomic signature can be used to assist clinicians to predict LN metastasis non-invasively.

Radiomics can convert digital medical images to mineable data, and analyze this data to improve detection, diagnosis, stage, and prediction power. Radiomics may help to answer questions

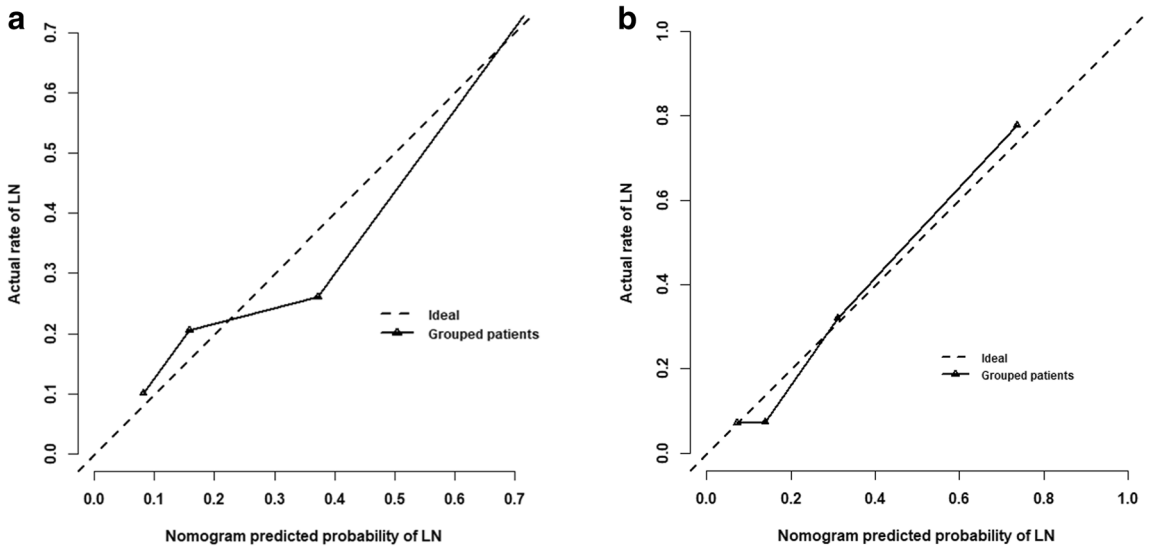

Fig. 4 **a**, **b** Calibration curve of the nomogram for the training cohort and validation cohort. The calibration curve was used to show the relationship between the predicted value and the true value. The *X*-axis represents the probability that nomogram predicted the LN metastasis, while *Y*-axis represents actual rate of LN metastasis. The dotted line in the middle represents the perfect prediction, and the solid line represents the predictive power of the nomogram. The closer the solid line is to the dotted line, the better the predictive power of the model

like whether existence of ALNM or the number of metastatic LNs, and this may affect breast cancer patients' surgical strategy. In this study, we developed a radiomic signature based on features extracted from T1-DCE MRI, and the capability of the radiomic signature for estimating LN metastasis is impressing. The AUC, sensitivity, specificity, and accuracy were 0.78, 78%, 72%, and 70% in the validation cohort. This non-invasive method for assessing LNs only relied on MRI, and therefore, this method could serve as a routine examination for breast cancer. Furthermore, the sensitivity of the radiomic signature was higher than traditional MRI; the sensitivity and specificity of MRI for determining ALNM ranges from 37.1 to 88% and 73 to 96.7%, respectively [10, 11, 13, 15]. Although the radiomic signature is not as specific as MRI, the combination of them would be useful in clinical practice.

In our study, we found that many clinical characteristics were correlated with LN metastasis, including histological type, LN palpability, multifocality, and MRI-reported LN status. As expected, the variables associated with LN metastasis in this study were quite similar to other studies [29–31]. For example, Bevilacqua et al [29] assessed pathologic and clinical characteristics of SLNB patients, and found that age, tumor size, tumor type, tumor location, multifocality, lymphovascular invasion, and status of ER and PR were related with LN metastasis.

Taking into account the impact that clinical factors can have on LN metastasis, we developed a nomogram that incorporated radiomic signature, MRI-reported LN status, and LN palpation. We were encouraged that the nomogram showed excellent ability to evaluate LN metastases with an AUC of 0.87 in the validation cohort. Recently, a study [32] using radiomic methods to predict LN metastases in breast cancer patients was published (which, unlike ours, was based on T2 fat-suppression and diffusion-weighted sequences) which showed prediction performance that was slightly lower than ours. To date, there have been many studies [29, 31, 33] that have developed multivariate models for predicting LN metastasis based on clinical and histological information, compared to those studies, our greatest advantage is that LNs can be evaluated pre-operatively and without damage.

There are several limitations associated with this study. First, the radiomic signature and nomogram were based on features extracted from primary tumors instead of the LNs themselves. The reason is that it is difficult to match the LNs that have been biopsied or dissected was the LNs imaged on

Table 4 Metastatic LN number–related features

First-order feature	Shape feature	GLCM	GLSZM	GLRLM
Maximum	Major axis	Inverse difference normalized (IDN)	Large area high gray level emphasis (LAHGLE)	Long run low gray level emphasis (LRLGLE)
Skewness		Difference variance	Small area emphasis (SAE)	Gray level non-uniformity normalized (GLNN)
		Correlation		
		Autocorrelation		

GLCM gray level co-occurrence matrix, *GLSZM* gray level size zone matrix, *GLRLM* gray level run length matrix

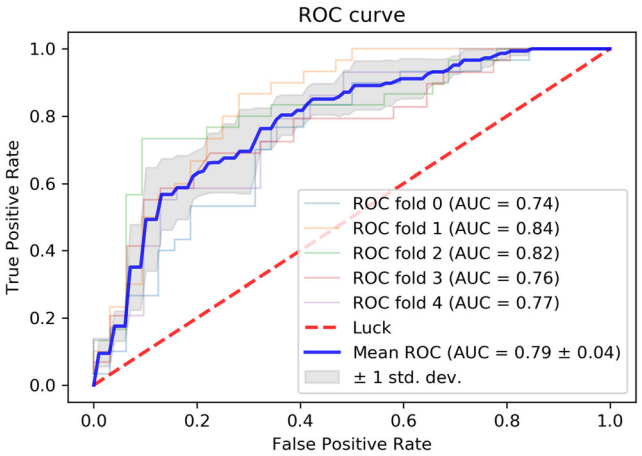

Fig. 5 ROC curve of radiomic signature for distinction the number of metastatic LNs (less than or equal to 2 and more than 2)

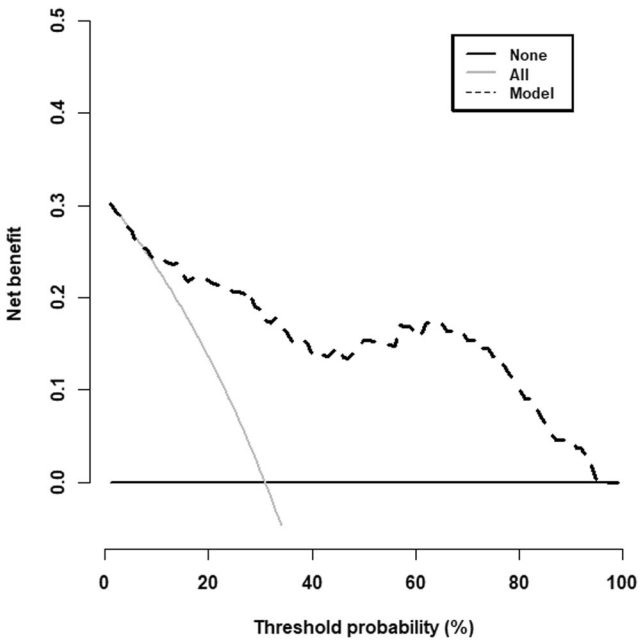

Fig. 6 Decision curve analysis of the radiomic nomogram. The *Y*-axis indicates net benefit to patients. The dotted line represents the nomogram, the gray line represents the hypothesis that all patients had LN metastasis, and the black line represents the hypothesis that no patients had LN metastasis. As demonstrated in the curve, when the threshold probability is between 0.12 and 0.95, the net benefit of using the radiomic nomogram to predict LN metastasis is greater than treat-all or treat-none scheme

MRI. In addition, we only cross-validated the radiomic signature for distinguishing the number of metastatic LNs, which was limited by the sample size. Independent validation in larger samples will be needed to develop high-level evidence needed for clinical use.

In conclusion, we developed a nomogram based on a radiomic signature, MRI-reported LN status, and LN palpability, it can be used to predict LN metastasis non-invasively, and the predictive profermance is good. We also tried to construct a radiomic signature to predict the number of metastatic LNs (less than 2 nodes/more than 2 nodes); it showed moderate predictive performance. Both nomogram and radiomic signature can be used as tools to assist clinicians in assessing LN metastasis in breast cancer patients.

Funding This study has received funding by Special Fund for Research in the Public Interest of China (201402020), National Key R&D Program of China (2017YFA0205200, 2017YFC1308700, 2017YFC1308701, 2017YFC1309100, 2016YFC0103803), National Natural Science Foundation of China (81227901, 81771924, 81501616, 81671851, 81671854, and 81527805), the Beijing Natural Science Foundation (L182061), the Bureau of International Cooperation of Chinese Academy of Sciences (173211KYSB20160053), the Science and Technology Service Network Initiative of the Chinese Academy of Sciences (KFJ-SW-STS-160), the Beijing Municipal Science and Technology Commission (Z171100000117023, Z161100002616022), the Instrument Developing Project of the Chinese Academy of Sciences (YZ201502), and the Youth Innovation Promotion Association CAS (2017175).

Compliance with ethical standards

Guarantor The scientific guarantor of this publication is Yahong Luo.

Conflict of interest The authors of this manuscript declare no relationships with any companies, whose products or services may be related to the subject matter of the article.

Statistics and biometry One of the authors has significant statistical expertise.

Informed consent Written informed consent was waived by the Institutional Review Board.

Ethical approval Institutional Review Board approval was obtained.

Methodology
- retrospective
- diagnostic study
- performed at one institution

References

1. Ferlay J, Soerjomataram I, Dikshit R et al (2015) Cancer incidence and mortality worldwide: sources, methods and major patterns in globocan 2012. Int J Cancer 136:E359
2. Lu S, Huang X, Yu H et al (2016) Dietary patterns and risk of breast cancer in Chinese women: a population-based case-control study. Lancet 388:S61
3. Weigel MT, Dowsett M (2010) Current and emerging biomarkers in breast cancer: prognosis and prediction. Endocr Relat Cancer 17: R245–R262
4. Gherghe M, Bordea C, Blidaru A (2015) Sentinel lymph node biopsy (SLNB) vs axillary lymph node dissection (ALND) in the current surgical treatment of early stage breast cancer. J Med Life 8: 176–180
5. Sakorafas GH, Peros G, Cataliotti L, Vlastos G (2006) Lymphedema following axillary lymph node dissection for breast cancer. Surg Oncol 15:153–165
6. Warmuth MA, Bowen G, Prosnitz LR et al (2015) Complications of axillary lymph node dissection for carcinoma of the breast. Cancer 83:1362–1368
7. McMasters KM, Tuttle TM, Carlson DJ et al (2000) Sentinel lymph node biopsy for breast cancer: a suitable alternative to routine axillary dissection in multi-institutional practice when optimal technique is used. J Clin Oncol 18:2560–2566
8. Schrenk P, Rieger R, Shamiyeh A, Wayand W (2000) Morbidity following sentinel lymph node biopsy versus axillary lymph node dissection for patients with breast carcinoma. Cancer 88:608–614
9. Kvistad KA, Rydland J, Smethurst HB, Lundgren S, Fjøsne HE, Haraldseth O (2000) Axillary lymph node metastases in breast cancer: preoperative detection with dynamic contrast-enhanced MRI. Eur Radiol 10:1464–1471
10. Valente SA, Levine GM, Silverstein MJ et al (2012) Accuracy of predicting axillary lymph node positivity by physical examination, mammography, ultrasonography, and magnetic resonance imaging. Ann Surg Oncol 19:1825–1830
11. An YS, Lee DH, Yoon JK et al (2014) Diagnostic performance of 18F-FDG PET/CT, ultrasonography and MRI detection of axillary lymph node metastasis in breast cancer patients. Nuklearmedizin 53:89–94
12. Zhang YN, Wang CJ, Xu Y et al (2015) Sensitivity, specificity and accuracy of ultrasound in diagnosis of breast cancer metastasis to the axillary lymph nodes in Chinese patients. Ultrasound Med Biol 41:1835–1841
13. Hwang SO, Lee SW, Kim HJ, Wan WK, Park HY, Jin HJ (2013) The comparative study of ultrasonography, contrast-enhanced MRI, and 18F-FDG PET/CT for detecting axillary lymph node metastasis in T1 breast cancer. J Breast Cancer 16:315–321
14. Diepstraten SC, Sever AR, Buckens CF et al (2014) Value of preoperative ultrasound-guided axillary lymph node biopsy for preventing completion axillary lymph node dissection in breast cancer: a systematic review and meta-analysis. Ann Surg Oncol 21:51–59
15. Cooper KL, Meng Y, Harnan S et al (2011) Positron emission tomography (PET) and magnetic resonance imaging (MRI) for the assessment of axillary lymph node metastases in early breast cancer: systematic review and economic evaluation. Health Technol Assess 15:1–134
16. Pilewskie M, Morrow M (2014) Applications for breast magnetic resonance imaging. Surg Oncol Clin N Am 23:431–449
17. Mainiero MB, Lourenco A, Mahoney MC et al (2013) ACR appropriateness criteria breast cancer screening. J Am Coll Radiol 10:11–14
18. Gillies RJ, Kinahan PE, Hricak H (2016) Radiomics: images are more than pictures, they are data. Radiology 278:563–577
19. Yip SS, Aerts HJ (2016) Applications and limitations of radiomics. Phys Med Biol 61:R150–R166
20. Lambin P, Rios-Velazquez E, Leijenaar R et al (2012) Radiomics: extracting more information from medical images using advanced feature analysis. Eur J Cancer 48:441–446

21. Bickelhaupt S, Paech D, Kickingereder P et al (2017) Prediction of malignancy by a radiomic signature from contrast agent-free diffusion MRI in suspicious breast lesions found on screening mammography. J Magn Reson Imaging 46(2):604–616
22. Chang RF, Chen HH, Chang YC, Huang CS, Chen JH, Lo CM (2016) Quantification of breast tumor heterogeneity for ER status, HER2 status, and TN molecular subtype evaluation on DCE-MRI. Magn Reson Imaging 34:809–819
23. Fan M, Wu G, Cheng H, Zhang J, Shao G, Li L (2017) Radiomic analysis of DCE-MRI for prediction of response to neoadjuvant chemotherapy in breast cancer patients. Eur J Radiol 94:140–147
24. Giuliano AE, Hunt KK, Ballman KV et al (2017) Axillary dissection vs no axillary dissection in women with invasive breast cancer and sentinel node metastasis: a randomized clinical trial. JAMA 305:569–575
25. Lyman GH, Temin S, Edge SB et al (2014) Sentinel lymph node biopsy for patients with early-stage breast cancer: American society of clinical oncology clinical practice guideline update. J Clin Oncol 32:1365–1383
26. Kim EJ, Kim SH, Kang BJ, Choi BG, Song BJ, Choi JJ (2014) Diagnostic value of breast MRI for predicting metastatic axillary lymph nodes in breast cancer patients: diffusion-weighted MRI and conventional MRI. Magn Reson Imaging 32:1230–1236
27. van Griethuysen JJM, Fedorov A, Parmar C et al (2017) Computational radiomics system to decode the radiographic phenotype. Cancer Res 77:e104–e107
28. Lakhani SR, Ellis IO, Schnitt SJ, Tan PH, van de Vijver MJ (2012) WHO classification of tumours of the breast. International Agency for Research on Cancer, Lyon
29. Bevilacqua JL, Kattan MW, Fey JV, Cody HS 3rd, Borgen PI, Van Zee KJ (2007) Doctor, what are my chances of having a positive sentinel node? A validated nomogram for risk estimation. J Clin Oncol 25:3670–3679
30. Viale G, Zurrida S, Maiorano E et al (2005) Predicting the status of axillary sentinel lymph nodes in 4351 patients with invasive breast carcinoma treated in a single institution. Cancer 103:492–500
31. Wu JL, Tseng HS, Yang LH et al (2014) Prediction of axillary lymph node metastases in breast cancer patients based on pathologic information of the primary tumor. Med Sci Monit 20:577–581
32. Dong Y, Feng Q, Yang W et al (2018) Preoperative prediction of sentinel lymph node metastasis in breast cancer based on radiomics of T2-weighted fat-suppression and diffusion-weighted MRI. Eur Radiol 28:582–591
33. Xie F, Yang H, Wang S et al (2012) A logistic regression model for predicting axillary lymph node metastases in early breast carcinoma patients. Sensors (Basel) 12:9936–9950